Journal of Comparative Physiology B
https://doi.org/10.1007/s00360-023-01528-y

ORIGINAL PAPER

Activation of oxytocinergic neurons enhances torpor in mice

Maia T. Hare[1,2] · Matthew E. Carter[1] · Steven J. Swoap[1]

Received: 24 September 2023 / Revised: 13 November 2023 / Accepted: 20 November 2023

Abstract

Mus musculus enters a torpid state in response to caloric restriction in sub-thermoneutral ambient temperatures. This torpid state is characterized by an adaptive and controlled decrease in metabolic rate, heart rate, body temperature, and activity. Previous research has identified the paraventricular nucleus (PVN) within the hypothalamus, a region containing oxytocin neurons, as a location that is active during torpor onset. We hypothesized that oxytocin neurons within the PVN are part of this neural circuit and that activation of oxytocin neurons would deepen and lengthen torpor bouts. We report that activation of oxytocin neurons alone is not sufficient to induce a torpor-like state in the fed mouse, with no significant difference in body temperature or heart rate upon activation of oxytocin neurons. However, we found that activation of oxytocin neurons prior to the onset of daily torpor both deepens and lengthens the subsequent bout, with a 1.7 ± 0.4 °C lower body temperature and a 135 ± 32 min increase in length. We therefore conclude that oxytocin neurons are involved in the neural circuitry controlling daily torpor in the mouse.

Keywords Torpor · Hibernation · Oxytocin · Chemogenetics · Fasting

Introduction

The laboratory mouse, *Mus musculus,* adapts to periods of food scarcity by entering daily torpor, a state characterized by temporary decreases in metabolic rate (MR), heart rate (HR), core body temperature (T_B), and physical activity that is seen in many species of small mammals and birds (Geiser and Ruf 1995; Hudson and Scott 1979; Ruf and Geiser 2015). Torpor is an adaptive state of controlled and reversible metabolic depression (Melvin and Andrews 2009). Because the torpid MR is typically not sufficient to maintain normal T_B, mice entering a torpid state exhibit a sharp decrease in T_B towards ambient room temperature (T_A) (Swoap and Gutilla 2009). The autonomic nervous system is intimately involved in the induction of torpor. The parasympathetic nervous system drives the bradycardia and increased HR variability observed during the onset of torpor (Milsom et al. 2001; Morhardt 1970; Swoap and Gutilla 2009; Vicent et al. 2017). In addition, an intact sympathetic nervous system is required for the torpor phenotype (Braulke and Heldmaier 2010; Swoap and Weinshenker 2008) and is responsible for the increase in total peripheral resistance (Hudson and Scott 1979; Swoap and Gutilla 2009) as well as activation of white fat, decrease in circulating leptin levels, and increase in lipolysis that occur with fasting and torpor (Swoap et al. 2006).

While the physiological consequences of the autonomic dynamics surrounding a torpor bout are well characterized in many small mammals including the laboratory mouse, the neural circuitry in the brain involved in torpor initiation, maintenance, and arousal remain unclear. Regions within the central nervous system that have autonomic and thermoregulatory roles may be important in the potential neural circuitry controlling torpor. Recent research has identified candidate regions within the hypothalamus that may be involved with daily torpor in the mouse (Ambler et al. 2022; Hrvatin et al. 2020; Takahashi et al. 2022, 2020; Yang et al. 2023; Zhang et al. 2020). The preoptic area (POA) of the hypothalamus (POA), a key coordinator of mammalian thermoregulation (Nakamura and Shaun 2008; Tan et al. 2016), is required for entry into fasting-induced torpor in mice (Zhang et al.

Communicated by G.Heldmaier.

✉ Steven J. Swoap
sswoap@williams.edu

[1] Department of Biology, Williams College, Williamstown, MA 01267, USA

[2] Present Address: Zucker School of Medicine at Hofstra/Northwell, 500 Hofstra Blvd, Hempstead, NY 11549, USA

Published online: 03 January 2024

2020). Furthermore, activation of the POA induces long bouts of hypometabolism and hypothermia (Hrvatin et al. 2020; Takahashi et al. 2020; Zhang et al. 2020). The POA receives nutritional status information from the arcuate nucleus (ARC) and circadian information from the suprachiasmatic nucleus (SCN), providing an anatomical link between nutritional status, circadian rhythms, and thermoregulation (Guzman-Ruiz et al. 2015). The dorsal medial hypothalamus (DMH) is also likely involved in the neural pathway given that projections from the POA to the DMH are involved with thermoregulation (Tan et al. 2016; Zhao et al. 2017), the DMH is active during torpor (Hitrec et al. 2019), and reactivation of neurons within the DMH prolongs and deepens fasting-induced torpor in the mouse (Ambler et al. 2022). The hypothalamic paraventricular nucleus (PVN) also receives projections from the POA (Dergacheva et al. 2016). The potential role of the PVN in the neural circuit controlling torpor has received little investigation to date.

The PVN contains oxytocin (OXT), vasopressin (AVP), and corticotropic releasing hormone (CRH) neurons and plays an important role in control of the autonomic nervous system and thermoregulation, for example playing an active role in the inhibition of sympathetic outflow to brown adipose tissue (Dos-Santos et al. 2018; Ferguson et al. 2008; Madden and Morrison 2009). Bilateral ablation of the PVN inhibits both torpor and circadian rhythms in Siberian hamsters (Norman 1995). In addition, activation of OXT neurons found in the PVN decreases the high BP and HR seen in rats subject to intermittent hypoxia, showing that this population of OXT neurons is capable of promoting some of the physiological features of torpor such as cardiovascular depression (Garrott et al. 2017; Jameson et al. 2016). Given that the PVN receives projections from the ARC and POA (Bouret et al. 2004; Dergacheva et al. 2017) and contains OXT neurons involved in the regulation of the parasympathetic nervous system and cardiovascular depression (Dergacheva et al. 2016; Jurek and Neumann 2018; Ming Sheng Zhou 2014), we reasoned that the OXT neurons within the PVN may play an important role in torpor initiation in the mouse. We first hypothesize that OXT neurons in the PVN are active during torpor. Further, we hypothesize that activation of OXT neurons via DREADDs (designer receptors exclusively activated by designer drugs) in a fasted mouse will initiate a torpor bout and will lengthen/deepen the bout.

Methods

Housing

Male (~30 g) and female (~25 g) 3-month old mice were singly housed on a 12-h light:dark cycle. Prior to experimentation, mice were housed at 22 °C and given food and water ad libitum. All housing and protocols associated with this experiment were approved and overseen by the Williams College Institutional Animal Care and Use Committee.

Telemetry

Mice were implanted with either temperature or electrocardiogram (ECG) telemetry devices at least 1 week prior to the start of the experiment. Temperature telemetry devices (TA-F10; Data Sciences International) returning T_B and activity were placed in the peritoneal cavity. After surgery, data was recorded for 1 s at a rate of once per minute for the duration of the experiment. ECG telemetry devices (ETA-F20; Data Sciences International) returning HR, T_B, and activity were implanted in the peritoneal cavity and sutured into the body wall. ECG leads were placed subcutaneously on either side of the heart and sutured into place. After surgery, waveforms from the implanted telemeters were recorded for 10 s intervals at a sampling rate of 500 Hz, once per minute.

Mice were additionally implanted with intraperitoneal catheters for needleless drug delivery. Catheters were constructed out of 0.43 × 0.94 mm polyurethane tubing (Instech, VAHBPU-T25). The tip of the catheter was secured intraperitoneally and the body of the catheter was tunneled subcutaneously to the back of the neck where it was connected to a mouse vascular access button (Instech, VABM1B/22). At least 1 week post-surgery, the button was connected to an external 0.38 × 1.09 mm polyethylene catheter (Instech, BTPE-20) to allow for IP injections with minimal disruption to the mice. The catheter was secured to a swivel (Instech, 375/25PS) to allow the mice to move freely about the cage.

Perfusion

Following experimental procedures, mice were anesthetized with an IP injection of 250 mg/kg Avertin (2,2,2 tribromoethanol (Sigma-Aldrich, Product #T48402) dissolved in Tert-amyl alcohol and sterile saline). Mice were then transcardially perfused with 0.01 M PBS, followed by 4% paraformaldehyde in PBS. Brains were extracted, fixed overnight in 4% paraformaldehyde at 4 °C, and cryoprotected in 30% sucrose dissolved in PBS for an additional 24 h at 4 °C. Each brain was sectioned at 30 µm thickness on a microtome (Leica Microsystems) and stored in cold PBS prior to immunohistochemistry.

Immunohistochemistry

For all immunohistochemistry analysis, sections were washed in PBS followed by PBS with 0.2% Triton X-100

(PBST) for 10 min each at room temperature. Sections were then incubated in a blocking solution composed of PBST with 3% normal donkey serum (Jackson ImmunoResearch, 017-000-121) for 15 min at room temperature. Sections were incubated in primary antibody in blocking solution overnight at 4 °C. After three 5-min washes in PBST and one 5-min wash in blocking solution, sections were incubated in the secondary antibody in blocking solution for 1 h at room temperature. Sections were washed three times in PBS for 5 min before mounting onto SuperFrost Plus glass slides (VWR, 48311-703), and coverslipped with Dapi Fluoromount-G (Southern Biotech, 0100-20). Slides were imaged using an Eclipse 80i epifluorescent microscope (Nikon), and images were captured using a RETIGNA 2000R digital camera. Images were colored using Photoshop CS5 (Adobe Systems).

Characterization of PVN activity during torpor

We crossed female *R26-stop-EYFP* mice (Jackson Laboratories, Catalog #006148) bred on a C57Bl/6J background with male *Oxytocin*$^{Cre/+}$ mice (Jackson Laboratories, Catalog #024234) bred on a C57Bl/6J background to create *Oxytocin*^{YFP} mice. Because the *Oxytocin*$^{Cre/+}$ mice were heterozygotes, half of the offspring expressed YFP in OXT neurons.

To assess whether OXT neurons in the PVN are active during torpor, mice were calorically restricted at 70% of normal food intake at an T_A of 20 °C, a protocol that induced torpor bouts around the third day of restricted food intake. Mice were euthanized and perfused on day 5 of this experiment, 2 h after the initial drop in T_B as measured by internal temperature telemeters. Two groups of mice served as non-torpid controls: mice fed at a T_A of 20 °C, and mice fasted at a T_A of 30 °C. Neither of these sets of control mice entered torpor and were perfused at the same time of day as torpid mice. Male mice were selected for this experiment for consistency in torpor induction and bouts. Brain sections were incubated in rabbit anti-Fos (1:1000; Cell Signaling Technology, 2250) for primary exposure and AlexaFluor 594 donkey anti-rabbit (1:250; Jackson ImmunoResearch, 711-545-152) for secondary exposure.

Fos protein staining within the PVN was quantified, as a measure of activated neurons, by a blinded investigator by counting Fos + cells per section from ~ − 1.30 to − 0.60 mm from bregma (six sections per mouse). Quantification of colocalization of Fos and YFP (marking oxytocinergic (OXT) cells) in the PVN followed the same procedure as above, counting Fos + cells, YFP + cells, and overlap between these cells.

Chemogenetic activation of OXT neurons

We crossed female *R-26-LSL-hM3Dq-DREADD* mice (Jackson Laboratories, Catalog #026220) bred on a C57Bl/6J background with male *Oxytocin*$^{Cre/+}$ mice bred on a C57Bl/6J background to create *Oxytocin*$^{hM3Dq+}$ mice. Because the *Oxytocin*$^{Cre/+}$ mice were heterozygotes for *Cre*, the offspring either expressed DREADD receptors in OXT neurons (*Oxytocin*$^{hM3Dq+}$) or there was no expression (*Oxytocin*$^{hM3Dq-}$) and these mice served as controls. Experimenters did not know the genotype of the mice (*Oxytocin*$^{hM3Dq+}$ vs. *Oxytocin*$^{hM3Dq-}$) until after experimentation was complete when the mice were euthanized, and immunohistochemistry was performed to learn the genotype of the mice. Mice were identified as either (*Oxytocin*$^{hM3Dq+}$; $n = 5$ females; $n = 2$ males) or there was no expression (*Oxytocin*$^{hM3Dq-}$; $n = 4$ females; $n = 2$ males). The telemetry-implanted mice were injected IP through the indwelling catheter with either saline or 0.1 mg/kg of the DREADD ligand clozapine N-oxide (CNO) diluted in saline while fully fed with a randomized cross-over design. Injections were spaced with at least one day recovery period in between control saline and CNO injection days. First, fully fed mice received injections 10–40 min into the light phase at an ambient temperature of 20 °C. The timing of these injections was such that mice would be in their resting phase, and a time when torpor is manifest in the fasted mouse (van der Vinne et al. 2018). Next, mice were calorically restricted at 70% of their normal food intake at 20 °C, a protocol that induced torpor bouts around the third day of restricted food intake. Five days after the start of caloric restriction, mice were injected between 1.5 and 2 h before the anticipated torpor bout, which was approximately 6–6.5 h into the dark phase.

After the end of experimentation, animals were refed, receiving food ad libitum for 3 + days. A subset of male and female mice were injected with CNO and perfused 2 h following injection as proof of principle that CNO injection resulted in activation in the PVN. Brain sections were incubated in rabbit anti-Fos for primary exposure and AlexaFluor 594 donkey anti-rabbit for secondary exposure. Fos in the PVN was quantified by a blinded investigator by counting Fos + cells per section from ~ − 1.30 to − 0.60 mm from bregma (4 sections per mouse).

After all experimentation was complete, immunohistochemistry was performed to identify which mice were *Oxytocin*$^{hM3Dq+}$ and which were *Oxytocin*$^{hM3Dq-}$. Brain sections were incubated in rabbit HA-tag (1:1000; Cell Signaling Technology, C2954) for primary exposure and AlexaFluor 594 donkey anti-rabbit (1:250; Jackson ImmunoResearch, 711-585-152) for secondary exposure. Mice were designated *Oxytocin*$^{hM3Dq+}$ providing staining was clearly observed throughout the PVN.

Statistics

Results are reported as mean ± SE. Fos quantification was assessed by a one-way ANOVA followed by post-hoc LSD testing, with $p < 0.05$ taken as significant. Physiological parameters upon injection are assessed with repeated measures ANOVA. Individual ECG and temperature tracings and brain section images are representative.

Results

Fos staining of the PVN provides a snapshot of the neural state during torpor onset (Fig. 1A). The PVN had significantly more Fos + cells per brain section in mice entering torpor ($n = 3$, 54 ± 24) than in non-torpid cold ($n = 3$, 1.2 ± 0.5) and fasted ($n = 3$, 1.8 ± 0.6) control mice; $t(4) = 2.2333$, $p = 0.0446$; $t(4) = 2.2079$, $p = 0.0459$ (Fig. 1B, C). Preliminary results suggest that the active neurons seen in the PVN during torpor is specifically in OXT neurons (Fig. S1).

We next generated mice expressing modified forms of human M3 muscarinic receptors that can be activated by CNO specifically in OXT neurons (*Oxytocin*$^{hM3Dq+}$ mice). One hour post CNO injection, an average of 27 ± 9.5 Fos + cells/brain section were present in the PVN of *Oxytocin*$^{hM3Dq+}$ mice ($n = 3$), while 0.42 ± 0.30 Fos + cells/section were present in that of *Oxytocin*$^{hM3Dq-}$ control mice ($n = 3$); $t(4) = 2.7437$, $p = 0.0259$ (Fig. 2).

To determine whether chemogenetic activation of OXT neurons influences baseline body temperature or HR, we compared injection of saline and CNO in fully fed *Oxytocin*$^{hM3Dq+}$ mice and *Oxytocin*$^{hM3Dq-}$ control mice at 20 °C. Mixed model ANOVA revealed no main effect of CNO on T_B ($F(1, 11) = 1.309$, $p = 0.277$) or HR ($F(1, 5) = 0.656$, $p = 0.455$) over the 8 h following injection (Table 1). In addition, there was no main effect of genotype on T_B ($F(1, 11) = 0.112$, $p = 0.744$) or HR ($F(1, 5) = 0.960$, $p = 0.372$).

We next sought to determine whether activation of OXT neurons prior to a bout of torpor influenced the ensuing torpor bout. Torpid T_B upon injection of CNO or saline was measured over the 8 h following injection in *Oxytocin*$^{hM3Dq+}$ ($n = 7$) and *Oxytocin*$^{hM3Dq-}$ ($n = 6$) mice. Activation of OXT neurons in mice experiencing regular daily torpor bouts influenced the depth and length of the ensuing torpor bout (Figs. 3, 4). Mixed model ANOVA revealed a main effect of CNO on average torpid T_B; $F(1,$

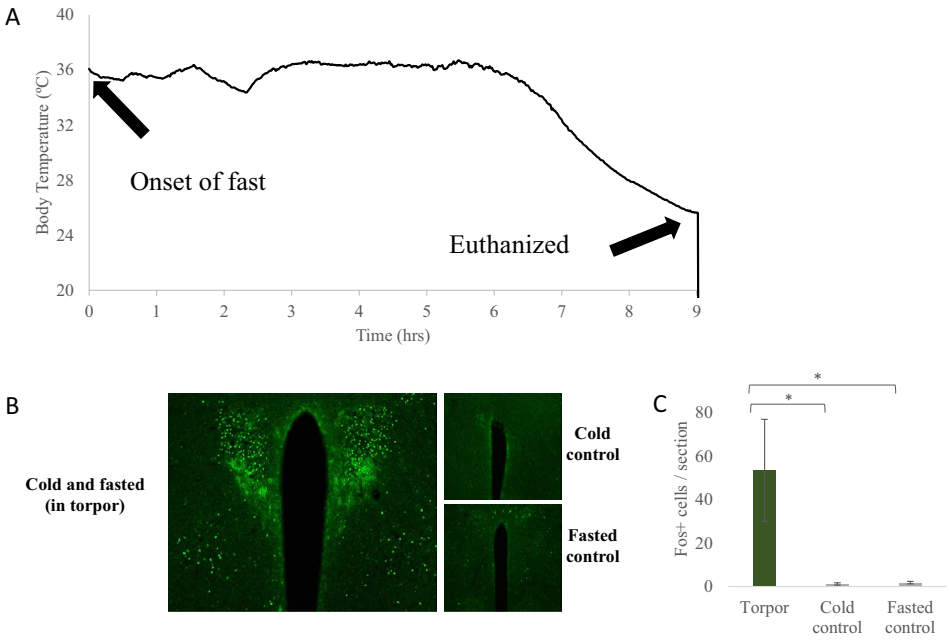

Fig. 1 Neurons within the paraventricular nucleus (PVN) are active during torpor onset. **A** Typical tracing of body temperature is shown for a representative mouse in the torpid condition. Euthanasia of this mouse occurred ~ 9 h after initiation of the fast. **B** Typical brain sections showing Fos + cells in the paraventricular nucleus of a fasted mouse at 20 °C that had entered torpor, a fed mouse at 20 °C (cold control), and a fasted mouse at 30 °C (fasted control). Sections were taken between − 1.30 and − 0.60 mm from bregma. **C** The number of Fos + cells were counted for each group ($n = 3$ per group, 6 sections per mouse). Torpid mice had significantly more Fos + staining than control mice animals when compared using a one-way ANOVA followed by a post-hoc LSD test, with $p < 0.05$ taken as significant (indicated by *). Standard error bars are shown

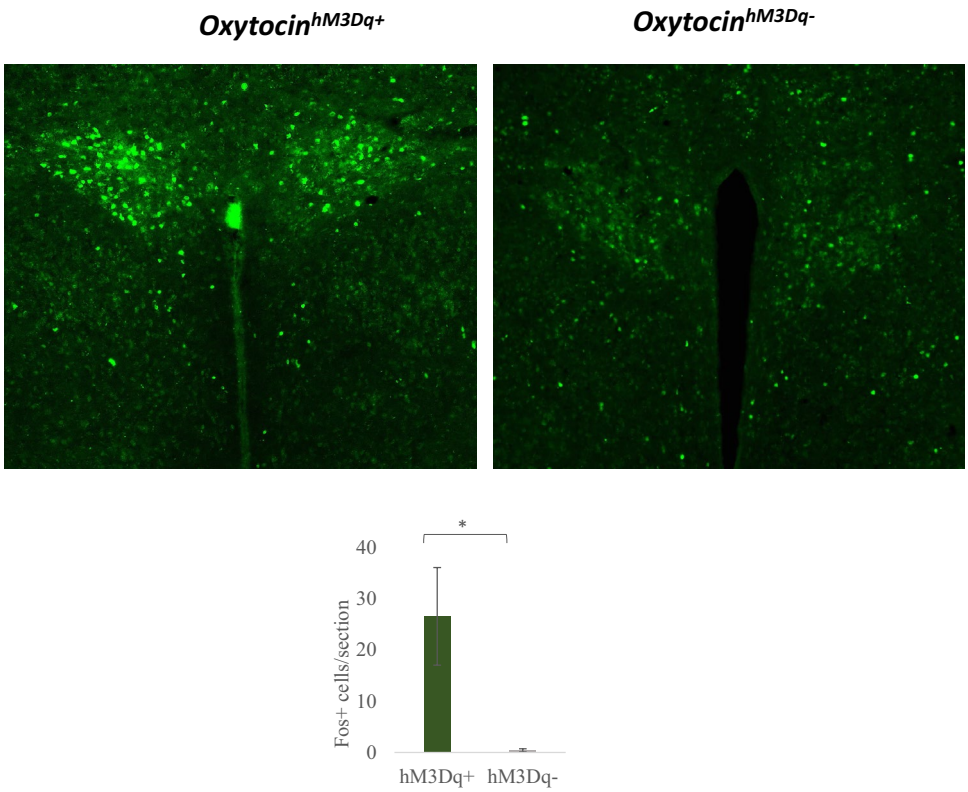

Fig. 2 CNO injection activates OXT neurons in the PVN through *hM3Dq*–mediated excitation. *Oxytocin*$^{hM3Dq+}$ and *Oxytocin*$^{hM3Dq-}$ mice were generated by breeding *R-26-LSL-hM3Dq-DREADD* with *Oxytocin*$^{Cre/+}$ mice. Mice ($n=3$ per group) were injected with CNO (0.1 mg/kg) and euthanized 60 min after injection. Sections in the PVN were then stained for Fos. *Oxytocin*$^{hM3Dq+}$ mice had significantly more Fos + cells in the PVN than *Oxytocin*$^{hM3Dq-}$ controls when compared using Student's *t* tests with $p<0.05$ taken as significant (indicated by *). Standard error bars are shown

Table 1 CNO injection does not affect average body temperature or heart rate in fully fed mice

	Body temperature				Heart rate			
	N	Mean (SE)	95% CI	*p*	*N*	Mean (SE)	95% CI	*p*
Oxytocin^{hM3Dq+}								
Saline	7	37.0 (0.18)	[36.6, 37.5]	0.3	4	609 (14)	[575, 646]	0.4
CNO		36.8 (0.17)	[36.4, 37.2]			615 (19)	[567, 663]	
Oxytocin^{hM3Dq-}								
Saline	6	36.7 (0.20)	[36.3, 37.2]	0.4	3	572 (16)	[530, 613]	0.4
CNO		36.6 (0.18)	[36.2, 37.0]			567 (21)	[512, 622]	

Average body temperature and heart rate were calculated for the 8 h immediately post-injection. Results are reported as mean (SE) and compared using Student's *t* tests with $p<0.05$ taken as significant

11) = 13.548, $p=0.004$. LSD post-hoc analysis showed that in *Oxytocin*$^{hM3Dq+}$ mice, injection of CNO resulted in a 1.7 °C ± 0.4 °C lower average torpid T_B than in saline-injected mice ($p=0.001$). There was also a main effect of CNO on minimum T_B; $F(1, 11)=7.086$, $p=0.022$. LSD post-hoc analysis revealed that in *Oxytocin*$^{hM3Dq+}$ mice, injection of CNO resulted in a 2.8 °C ± 0.9 °C lower minimum torpid T_B than in saline-injected mice ($p=0.003$). There was no significant difference in either average ($p=0.404$) or minimum T_B ($p=0.950$) between injection type in *Oxytocin*$^{hM3Dq-}$ control mice over the 8 h following injection.

CNO injection was additionally associated with increased torpor length, as measured as time spent below T_B of 30 °C. Repeated measure ANOVA revealed a main effect of CNO on torpor length; $F(1, 11)=10.411$, $p=0.008$. LSD post-hoc analysis revealed that in *Oxytocin*$^{hM3Dq+}$ mice, CNO injection increased length of torpor by 135 ± 32 min ($p=0.001$). There was no difference in length of torpor between injections in *Oxytocin*$^{hM3Dq-}$ control mice ($p=0.644$).

Torpid HR upon injection of CNO or saline was measured over the 8 h following injection in *Oxytocin*$^{hM3Dq+}$ ($n=4$) and *Oxytocin*$^{hM3Dq-}$ ($n=3$) mice experiencing daily torpor bouts. Mixed model ANOVA for a main effect of CNO showed no significant differences for average torpid HR ($F(1, 5)=4.999$, $p=0.076$) and minimum torpid HR ($F(1, 5)=5.059$, $p=0.074$. However, our planned LSD post-hoc analysis revealed that in *Oxytocin*$^{hM3Dq+}$ mice,

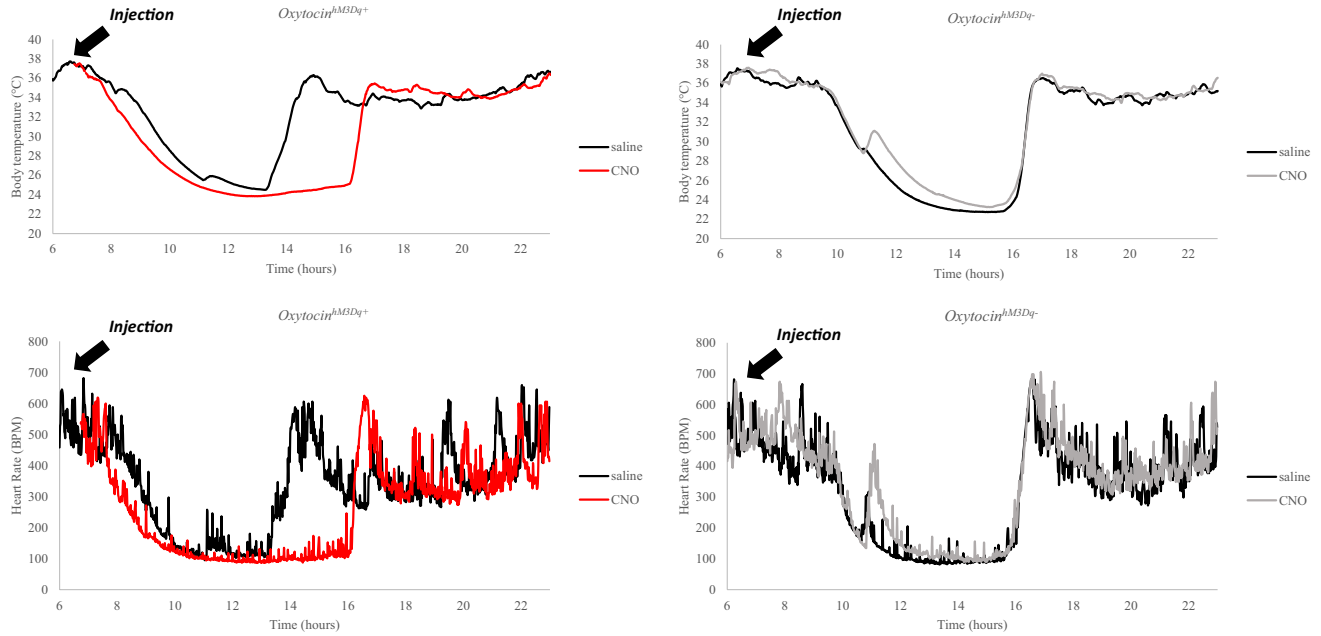

Fig. 3 OXT activation influences T_B and heart rate during torpor bouts. Typical T_B and heart rate tracings from two female mice, an *Oxytocin*$^{hM3Dq+}$ mouse and an *Oxytocin*$^{hM3Dq-}$ mouse, are shown. Mice were calorically restricted to 70% of normal food intake daily (at time 0 h) until the appearance of regular torpor bouts. On different days of caloric restriction mice were injected with either CNO (0.1 mg/kg) or saline as shown by the arrow, approximately 1 h before the anticipated onset of the torpor bout. Note the longer and deeper torpor bout with CNO in the *Oxytocin*$^{hM3Dq+}$ mouse

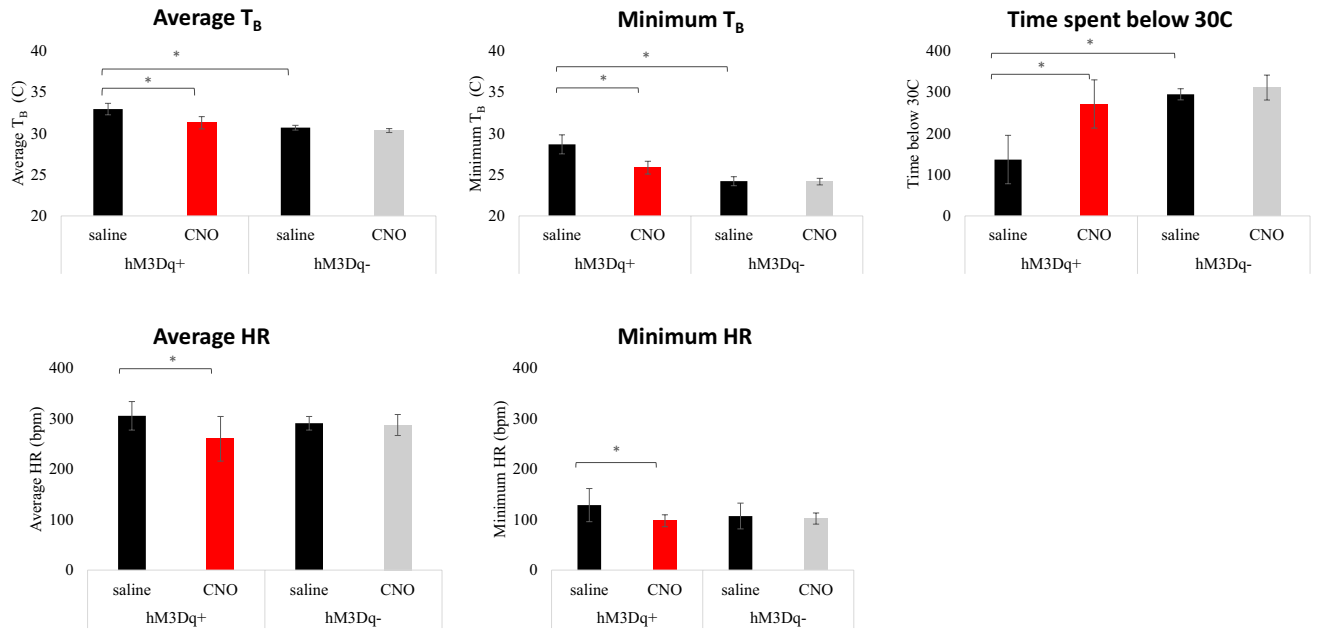

Fig. 4 OXT neuron activation decreases T_B and heart rate during torpor bouts. T_B and heart rate (HR) were averaged over a 12-h period, from hour 6 to hour 18 as shown in Fig. 3. Delivery of CNO lowered average T_B, average HR, minimum T_B, and minimum HR in *Oxytocin*$^{hM3Dq+}$ mice but not *Oxytocin*$^{hM3Dq-}$ mice. Similarly, torpor bouts were longer in *Oxytocin*$^{hM3Dq+}$ but not *Oxytocin*^{hM3Dq} mice after administration of CNO as assessed by the amount of time when T_B was below 30 °C. Physiological parameters are assessed with mixed measures ANOVA. Standard error bars are shown. Significance < 0.05 is indicated by *

CNO injection resulted in a 45.4 ± 14.3 BPM lower average torpid HR ($p = 0.025$) and 31.1 ± 10.5 BPM lower minimum torpid HR ($p = 0.031$) relative to saline-injected mice. There was no significant difference in average ($p = 0.845$) or minimum HR ($p = 0.699$) between injection type in *Oxytocin*$^{hM3Dq-}$ control mice.

The relationship between HR and T_B during hypothermia can be used to help differentiate natural torpor from non-natural torpor (Vicent et al. 2017). To compare OXT neuron enhanced torpor to natural torpor, we plotted HR as a function of T_B in OXT-activated torpor and in saline-control torpor (Fig. 5). The relationship between T_B and HR can be read clockwise from the top right corner: (1) initially, HR decreases prior to significant change in T_B, (2) T_B decreases as decrease in HR slows during onset of torpor, (3) HR increases prior to significant change in T_B, (4) T_B rises as increase in HR slows during arousal from torpor. In *Oxytocin*$^{hM3Dq+}$ mice, descent into OXT-enhanced torpor and ascent from the low T_B were qualitatively similar as to natural torpor with saline injections. To quantify this result, HR at T_B of 31 °C during descent and ascent in OXT-enhanced torpor was compared to that in saline-control torpor in a repeated measures ANOVA (Fig. 5B). There was no main effect of CNO on HR at a body temperature of 31 °C; $F(1, 3) = 5.348$, $p = 0.104$.

Discussion

The PVN plays important autonomic, thermoregulatory, and circadian roles (Dos-Santos et al. 2018; Norman 1995). Therefore, we hypothesized that neurons in this region would be involved in torpor, a state of rhythmic, autonomic-mediated reductions in MR, HR, and body temperature. Daily torpor in the mouse has an ultradian rhythm, occurring in periods less than 1 day, and disruption of ultradian rhythms in Djungarian hamsters prevents torpor (Braulke and Heldmaier 2010). Ultradian rhythms of 0.5–4 h originate in the PVN and subparaventricular zone and project to the SCN (Wu et al. 2018). Duration of ultradian firing in the PVN generally corresponds to that of torpor and is integrated with the circadian rhythm set by the SCN (van der Vinne et al. 2018). We show here that the PVN exhibits a significant increase in activity upon torpor onset in the laboratory mouse (Fig. 1), as has been seen previously (Hitrec et al. 2019). Further, given the cardiovascular depression that occurs during both torpor and OXT activation, we surmised that these OXT neurons within the PVN may be involved with daily torpor. Supporting this hypothesis, activation of OXT neuron activity in mice experiencing daily torpor bouts both deepened and lengthened those torpor bouts (Figs. 3, 4). Activation of OXT neurons in fully fed mice was not sufficient to induce torpor and did not affect baseline body temperature or HR (Table 1), suggesting that the effects of OXT activation on mouse physiology is torpor specific and requires input from additional brain regions. Taken together, OXT neurons in the PVN seem to play a modulatory role in the torpid phenotype.

While we focused here on OXT neurons within the PVN, several independent investigations have shown that activation of neuron types within the POA lead to some commonalities with natural daily torpor in the mouse that include a reduction in body temperature (Hrvatin et al. 2020; Takahashi et al. 2020, 2022; Yang et al. 2023; Zhang et al. 2020), a reduction in MR (Yang et al. 2023; Zhang et al. 2020), and a reduction in HR (Takahashi et al. 2022; Yang et al.

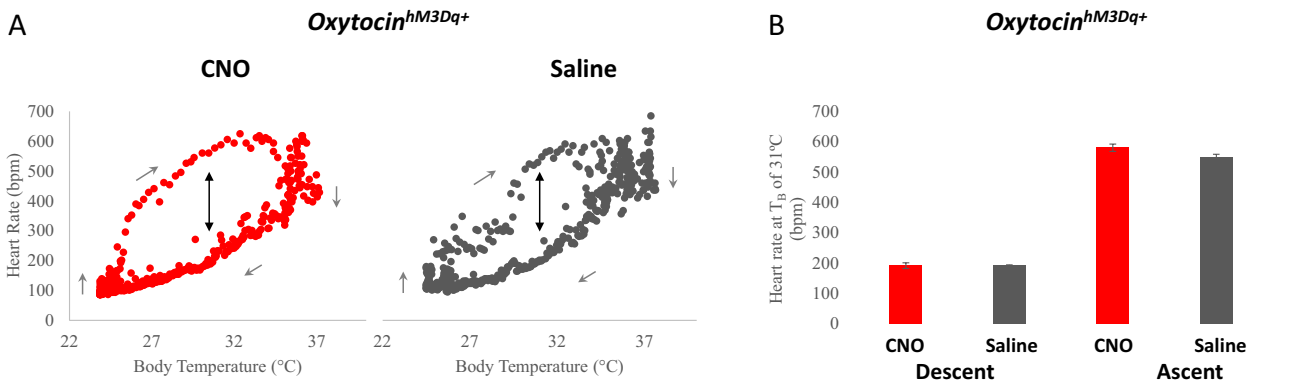

Fig. 5 OXT stimulated enhancement of torpor has the same qualitative and quantitative T_B/HR relationship as natural torpor. **A** HR is plotted as a function of concurrent T_B in a typical *Oxytocin*$^{hM3Dq+}$ mouse for two different torpor bouts, one with a CNO injection and the other with a saline injection. These hysteresis curves move in the direction as shown by the small arrows. **B** T_B /HR dynamics can be quantitively assessed by measuring HR at a T_B of 31 °C during descent and ascent from torpor, as indicated by the double-sided arrow in part A. Physiological parameters are assessed with repeated measures ANOVA. Standard error bars are shown. Significance < 0.05 is indicated by *

2023; Zhang et al. 2020). However, some of these investigations found bouts of induced hypothermia that lasted much longer than the lowered body temperature found in natural daily torpor in the mouse, which potentially calls to question whether the hypothermia in these studies is truly reflective of daily torpor or rather a failed regulation of body temperature (Hrvatin et al. 2020; Takahashi et al. 2020; Zhang et al. 2020). One potential clue towards this issue is assessing the interaction between multiple physiological measures, for example MR as a function of body temperature or HR as a function of body temperature. The dynamics between physiological measures during torpor entry and arousal can be informative. A time-delay in the change in body temperature relative to either the change in MR or HR during torpor entry and exit results in a hysteresis loop of characteristic shape and breadth (Geiser et al. 2014; Vicent et al. 2017). We have shown that the breadth of the hysteresis loop when plotting HR vs. T_B can differentiate between daily torpor and hypothermia (Vicent et al. 2017), while others have shown the directionality of the loop of MR vs. T_B can similarly differentiate between torpor and forced hypothermia (Geiser et al. 2014). One of the above-mentioned studies (Takahashi et al. 2022) found a hysteresis loop between HR and T_B, although no comparison to daily torpor was made. We show here that the HR and T_B relationship is unchanged between natural torpor and the deepened torpor with OXT stimulation (Fig. 5). The general deepening and lengthening of daily torpor in the mouse with OXT stimulation is similar in scope, but not as great in magnitude, as to those reported with stimulation of neurons within the DMH (Ambler et al. 2022). Given the multitude of connections, both direct and indirect, between the PVN and DMH, including those involved in caloric balance (Ambler et al. 2021), as well as both regions receiving projections from the POA (Bouret et al. 2004; Dergacheva et al. 2016; Tan et al. 2016), it may not be surprising that the physiological consequences of activating these regions results in qualitatively similar physiological outcomes. As POA-activated hypothermia share some of the characteristics of natural torpor, perhaps the added neural activity from the DMH and PVN will provide the missing input to recapitulate the torpid state.

The present study has some important limitations. The design of the present study activated all OXT neurons, including those populations outside of the PVN such as in the supraoptic nucleus (Jurek and Neumann 2018). We therefore cannot conclude that the OXT neurons within the PVN are solely responsible for the effects seen. Additional research specifically targeting OXT neurons in the PVN or subsets of OXT neurons within this region may shed light on the role this region plays in modulating torpor. Further, we cannot distinguish with the current data set whether the torpid state was lengthened, or that arousal was delayed. These two possibilities theoretically involve different circuits, with the former possibility being linked to active metabolic inhibition and the latter being linked to the circadian clock and timing of torpor. Given that the OXT-activated mice had deeper bouts of torpor (see Fig. 4), our data support the hypothesis that the torpid state was enhanced. However, we cannot be definitive in that conclusion without further evidence. In addition, while we cannot exclude the possibility that expression of DREADDs within OXT neurons affects the behavior of these neurons at baseline, to our knowledge, no study has demonstrated that expression of a DREADD transgene affects neural activity in the absence of administration of the agonist. While awareness of this potential is important when using DREADDs in the future, it does not change conclusions drawn from the present experiment as $Oxytocin^{hM3Dq+}$mice exhibited a significant enhancement of torpor when compared to their $Oxytocin^{hM3Dq-}$ control counterparts. Finally, while we showed that activation of OXT neurons enhances natural torpor, we did not investigate whether inhibition of these neurons prevents natural torpor, which would assess the necessity of this neuronal population in the neural network controlling torpor. While previous research has demonstrated the necessity of the PVN in Siberian hamsters (Norman 1995), future directions include investigating this question in the laboratory mice.

Supplementary Information The online version contains supplementary material available at https://doi.org/10.1007/s00360-023-01528-y.

Acknowledgements The authors thank the animal care staff for their assistance. Funds were provided by Williams College to SJS and MC.

Declarations

Conflict of interest The authors have no competing interests to declare that are relevant to the context of this article.

References

Ambler M, Hitrec T, Pickering A (2021) Turn it off and on again: characteristics and control of torpor. Wellcome Open Res 6:313. https://doi.org/10.12688/wellcomeopenres.17379.2

Ambler M, Hitrec T, Wilson A, Cerri M, Pickering A (2022) Neurons in the dorsomedial hypothalamus promote, prolong, and deepen torpor in the mouse. J Neurosci 42(21):4267–4277. https://doi.org/10.1523/JNEUROSCI.2102-21.2022

Bouret SG, Draper SJ, Simerly RB (2004) Formation of projection pathways from the arcuate nucleus of the hypothalamus to hypothalamic regions implicated in the neural control of feeding behavior in mice. J Neurosci 24(11):2797–2805. https://doi.org/10.1523/JNEUROSCI.5369-03.2004

Braulke LJ, Heldmaier G (2010) Torpor and ultradian rhythms require an intact signalling of the sympathetic nervous system. Cryobiology 60(2):198–203. https://doi.org/10.1016/j.cryobiol.2009.11.001

Dergacheva O, Yamanaka A, Schwartz AR, Polotsky VY, Mendelowitz D (2016) Direct projections from hypothalamic orexin neurons to brainstem cardiac vagal neurons. Neuroscience 339:47–53. https://doi.org/10.1016/j.neuroscience.2016.09.038

Dergacheva O, Yamanaka A, Schwartz AR, Polotsky VY, Mendelowitz D (2017) Optogenetic identification of hypothalamic orexin neuron projections to paraventricular spinally projecting neurons. Am J Physiol Heart Circ Physiol 312(4):H808–H817. https://doi.org/10.1152/ajpheart.00572.2016

Dos-Santos RC, Grover HM, Reis LC, Ferguson AV, Mecawi AS (2018) Electrophysiological effects of Ghrelin in the hypothalamic paraventricular nucleus neurons. Front Cell Neurosci 12:275. https://doi.org/10.3389/fncel.2018.00275

Ferguson AV, Latchford KJ, Samson WK (2008) The paraventricular nucleus of the hypothalamus—a potential target for integrative treatment of autonomic dysfunction. Expert Opin Ther Targets 12(6):717–727. https://doi.org/10.1517/14728222.12.6.717

Garrott K, Dyavanapalli J, Cauley E, Dwyer MK, Kuzmiak-Glancy S, Wang X, Mendelowitz D, Kay MW (2017) Chronic activation of hypothalamic oxytocin neurons improves cardiac function during left ventricular hypertrophy-induced heart failure. Cardiovasc Res 113(11):1318–1328. https://doi.org/10.1093/cvr/cvx084

Geiser F, Ruf T (1995) Hibernation versus daily torpor in mammals and birds: physiological variables and classification of torpor patterns. Physiol Zool 68(6):935–966

Geiser F, Currie SE, O'Shea KA, Hiebert SM (2014) Torpor and hypothermia: reversed hysteresis of metabolic rate and body temperature. Am J Physiol Regul Integr Comp Physiol 307(11):R1324-1329. https://doi.org/10.1152/ajpregu.00214.2014

Guzman-Ruiz MA, Ramirez-Corona A, Guerrero-Vargas NN, Sabath E, Ramirez-Plascencia OD, Fuentes-Romero R, Leon-Mercado LA, Basualdo Sigales M, Escobar C, Buijs RM (2015) Role of the suprachiasmatic and arcuate nuclei in diurnal temperature regulation in the rat. J Neurosci 35(46):15419–15429. https://doi.org/10.1523/JNEUROSCI.1449-15.2015

Hitrec T, Luppi M, Bastianini S, Squarcio F, Berteotti C, Lo Martire V, Martelli D, Occhinegro A, Tupone D, Zoccoli G, Amici R, Cerri M (2019) Neural control of fasting-induced torpor in mice. Sci Rep 9(1):15462. https://doi.org/10.1038/s41598-019-51841-2

Hrvatin S, Sun S, Wilcox OF, Yao H, Lavin-Peter AJ, Cicconet M, Assad EG, Palmer ME, Aronson S, Banks AS, Griffith EC, Greenberg ME (2020) Neurons that regulate mouse torpor. Nature 583(7814):115–121. https://doi.org/10.1038/s41586-020-2387-5

Hudson JW, Scott IM (1979) Daily torpor in the laboratory mouse, Mus musculus Var. Albino. Physiol Zool 52(2):205–218

Jameson H, Bateman R, Byrne P, Dyavanapalli J, Wang X, Jain V, Mendelowitz D (2016) Oxytocin neuron activation prevents hypertension that occurs with chronic intermittent hypoxia/hypercapnia in rats. Am J Physiol Heart Circ Physiol 310(11):H1549-1557. https://doi.org/10.1152/ajpheart.00808.2015

Jurek B, Neumann ID (2018) The oxytocin receptor: from intracellular signaling to behavior. Physiol Rev 98(3):1805–1908. https://doi.org/10.1152/physrev.00031.2017

Madden CJ, Morrison SF (2009) Neurons in the paraventricular nucleus of the hypothalamus inhibit sympathetic outflow to brown adipose tissue. Am J Physiol Regul Integr Comp Physiol 296(3):R831-843. https://doi.org/10.1152/ajpregu.91007.2008

Melvin RG, Andrews MT (2009) Torpor induction in mammals: recent discoveries fueling new ideas. Trends Endocrinol Metab 20(10):490–498. https://doi.org/10.1016/j.tem.2009.09.005

Milsom WK, Zimmer MB, Harris MB (2001) Vagal control of cardiorespiratory function in hibernation. Exp Physiol 86(6):791–796. https://doi.org/10.1111/j.1469-445x.2001.tb00046.x

Ming Sheng Zhou HS (2014) Cardiovascular action of oxytocin. J Autacoids. https://doi.org/10.4172/2161-0479.1000e124

Morhardt JE (1970) Heart rates, breathing rates and the effects of atropine and acetylcholine on white-footed mice (*Peromyscus* sp.) during daily torpor. Comp Biochem Physiol 33(2):441–457. https://doi.org/10.1016/0010-406x(70)90360-9

Nakamura KM, Shaun F (2008) A thermosensory pathway that controls body temperature. Nat Neurosci 11(1):62–71

Norman RF (1995) Paraventricular nucleus ablation disrupts daily torpor in Siberian hamsters. Brain Res Bull 37(2):193–198

Ruf T, Geiser F (2015) Daily torpor and hibernation in birds and mammals. Biol Rev Camb Philos Soc 90(3):891–926. https://doi.org/10.1111/brv.12137

Swoap SJ, Gutilla MJ (2009) Cardiovascular changes during daily torpor in the laboratory mouse. Am J Physiol Regul Integr Comp Physiol 297(3):R769-774. https://doi.org/10.1152/ajpregu.00131.2009

Swoap SJ, Weinshenker D (2008) Norepinephrine controls both torpor initiation and emergence via distinct mechanisms in the mouse. PLoS One 3(12):e4038. https://doi.org/10.1371/journal.pone.0004038

Swoap SJ, Gutilla MJ, Liles LC, Smith RO, Weinshenker D (2006) The full expression of fasting-induced torpor requires beta 3-adrenergic receptor signaling. J Neurosci 26(1):241–245. https://doi.org/10.1523/JNEUROSCI.3721-05.2006

Takahashi TM, Sunagawa GA, Soya S, Abe M, Sakurai K, Ishikawa K, Yanagisawa M, Hama H, Hasegawa E, Miyawaki A, Sakimura K, Takahashi M, Sakurai T (2020) A discrete neuronal circuit induces a hibernation-like state in rodents. Nature 583(7814):109–114. https://doi.org/10.1038/s41586-020-2163-6

Takahashi TM, Hirano A, Kanda T, Saito VM, Ashitomi H, Tanaka KZ, Yokoshiki Y, Masuda K, Yanagisawa M, Vogt KE, Tokuda T, Sakurai T (2022) Optogenetic induction of hibernation-like state with modified human Opsin4 in mice. Cell Rep Methods 2(11):100336. https://doi.org/10.1016/j.crmeth.2022.100336

Tan CL, Cooke EK, Leib DE, Lin YC, Daly GE, Zimmerman CA, Knight ZA (2016) Warm-sensitive neurons that control body temperature. Cell 167(1):47–59. https://doi.org/10.1016/j.cell.2016.08.028. (**e15**)

van der Vinne V, Bingaman MJ, Weaver DR, Swoap SJ (2018) Clocks and meals keep mice from being cool. J Exp Biol. https://doi.org/10.1242/jeb.179812

Vicent MA, Borre ED, Swoap SJ (2017) Central activation of the A1 adenosine receptor in fed mice recapitulates only some of the attributes of daily torpor. J Comp Physiol B 187(5–6):835–845. https://doi.org/10.1007/s00360-017-1084-7

Wu YE, Enoki R, Oda Y, Huang ZL, Honma KI, Honma S (2018) Ultradian calcium rhythms in the paraventricular nucleus and subparaventricular zone in the hypothalamus. Proc Natl Acad Sci USA 115(40):E9469–E9478. https://doi.org/10.1073/pnas.1804300115

Yang Y, Yuan J, Field RL, Ye D, Hu Z, Xu K, Xu L, Gong Y, Yue Y, Kravitz AV, Bruchas MR, Cui J, Brestoff JR, Chen H (2023) Induction of a torpor-like hypothermic and hypometabolic state in rodents by ultrasound. Nat Metab 5(5):789–803. https://doi.org/10.1038/s42255-023-00804-z

Zhang Z, Reis F, He Y, Park JW, DiVittorio JR, Sivakumar N, van Veen JE, Maesta-Pereira S, Shum M, Nichols I, Massa MG, Anderson S, Paul K, Liesa M, Ajijola OA, Xu Y, Adhikari A, Correa SM (2020) Estrogen-sensitive medial preoptic area neurons coordinate torpor in mice. Nat Commun 11(1):6378. https://doi.org/10.1038/s41467-020-20050-1

Zhao Z-DY, Wen Z, Gao C, Fu X, Zhang W, Zhoud Q, Chen W, Ni X, Lin J-K, Yang J, Xu X-H, Shen WL (2017) A hypothalamic circuit that controls body temperature. Proc Natl Acad Sci USA 114(9):E1755. https://doi.org/10.1073/pnas.1701881114